ELSEVIER

International Journal of Mass Spectrometry 182/183 (1999) 323–333

International Journal of Mass Spectrometry

Novel mixed ligand sandwich complexes: competitive binding of iron with benzene, coronene, and C_{60}

J.W. Buchanan, G.A. Grieves, J.E. Reddic, M.A. Duncan*

Department of Chemistry, University of Georgia, Athens, GA 30602, USA

Received 24 July 1998; accepted 10 September 1998

Abstract

Organometallic complexes of iron with benzene, coronene and C_{60} are produced in a molecular beam and studied with time-of-flight mass spectrometry and laser photodissociation. The cation complexes are produced in a pulsed nozzle laser vaporization source using an iron rod coated with a sublimed film of coronene and/or C_{60}. Benzene is seeded in the expansion gas. Masses of the form $[A_x–Fe–B_y]^+$ are observed when A and B are benzene, coronene, or C_{60}, taken any two at a time. Masses are observed for all combinations where $x + y = 1$ or 2, indicating the formation of monoligand and sandwich complexes. Mixed-ligand sandwiches form with comparable abundance to homoligand sandwiches. Mass-selected photodissociation probes the relative bonding strengths in these new species. (Int J Mass Spectrom 182/183 (1999) 323–333) © 1999 Elsevier Science B.V.

Keywords: Organometallic complexes; Metal ions; Photodissociation

1. Introduction

The unusual bonding exhibited by organometallic π complexes has been a subject of continuing interest for many years [1–4]. Of the π complexes studied, none have attracted as much fascination as sandwich species like ferrocene and dibenzene chromium. Many related organometallic species have been studied in the gas phase environment of mass spectrometers and/or molecular beams [5]. Metal benzene complexes or those with other small aromatic systems have generated particular interest for gas phase studies [2–20]. In recent developments in this area, Kaya and co-workers have produced remarkable multidecker sandwich complexes with benzene and substituted benzenes [21,22]. Bowers and co-workers [23] have investigated these species with "ion chromatography" and have confirmed that they have the multidecker sandwich structures proposed by Kaya and co-workers [21,22]. Metal complexes with involatile aromatic systems have also been produced, including polyaromatic hydrocarbons (PAHs) [24–26] and fullerenes [27–38]. In these experiments, laser or oven sources are required to produce the organics in the gas phase and to combine them with metal. Using such methods, Martin and co-workers have produced metal monolayer and even multilayer films on the surface of

* Corresponding author. E-mail: maduncan@arches.uga.edu

Dedicated to the memory of Ben Freiser to commemorate his many seminal contributions to mass spectrometry and gas phase ion chemistry.

PII S1387-3806(98)14239-2

C_{60} [33–36]. Our research group has investigated the photodissociation of M_x–C_{60}^+ species [37]. Kaya and co-workers have also generated metal–C_{60}–metal–C_{60} networks [38] which appear to be closely related to the multidecker sandwiches. These various species have exciting promise for the synthesis of new materials. However, the characterization of their structure and bonding remains a significant challenge.

Three recurring structural themes are suggested by these studies of new organometallic clusters. On the one hand, species such as fullerenes or PAHs have multiple aromatic ring sites where η_6 or η_5 π bonding can occur. Binding of metal atoms in these sites may produce structures resembling metal films. Filmlike structures have been indicated for metal–C_{60} and metal–C_{70} clusters [33–36] and for iron–coronene complexes [25]. If metal–metal bonding is preferred over metal-organic bonding, metal clusters may bind to organic species as a unit. Such "cluster-plus-cluster" structures have been suggested in the silver–C_{60} system [33–36] and in other transition metal–C_{60} systems [38]. A final possibility, which is perhaps more intriguing, is the formation of sandwiches or multidecker sandwiches. This behavior has been observed by Kaya and co-workers for transition metal species with benzene [21,22] and C_{60} [38]. Freiser and co-workers have reported M–$(C_{60})_2^+$ masses which are assumed to represent sandwich structures [27–30]. Dunbar and co-worker have observed similar stoichiometries for metal complexes with coronene ($C_{24}H_{12}$) [24]. In our own recent work, metal–coronene sandwiches are observed to be especially prominent in the case of iron complexes, where there is enhanced formation of $[Fe–cor_2]^+$ in both the distribution of clusters grown by the source and in the photofragmentation of larger clusters [25]. Multimetal atom sandwiches (e.g. $[Fe_3–cor_2]$) are also suggested in these data [25].

Although there have been many studies of organometallic complexes with volatile ligands, experiments with involatile ligands such as C_{60} and PAHs require the construction of more elaborate oven sources to sublime organic species into the gas phase [24,33–36]. However, our research group has recently demonstrated a method to incorporate involatile ligands into a pulsed nozzle laser vaporization source. We use metal rod samples coated with a thin film of the desired component. Thin films are applied in a separate sample preparation vacuum system, where a small oven source sublimes material onto the rod surface. The coated rod is then mounted in the molecular beam apparatus in the usual pulsed nozzle source configuration. Laser ablation of the film coated rod produces intact organic molecules and metal vapor in the gas phase and recombination of these species occurs in the growth channel region of the source. Only very stable molecules can survive the plasma conditions without fragmentation, but C_{60} and various polyaromatic hydrocarbon species satisfy this requirement. We have previously described the growth of various metal–C_{60} [37] and metal–PAH [25,26] species from this kind of source and have studied their photodissociation dynamics.

Previous experiments in our lab and others have produced metal ion sandwich complexes of iron with di-benzene [5–22], di-coronene [24–26] or di-C_{60} [27–37] ligands. These species form readily, but bond energies and specific gas phase structures have not been measured. The $[Fe–benzene]^+$ ion is the only relevant metal complex for which the binding energy has been measured and/or calculated by theory [13,14,17]. Motivated by the recent observation of sandwich clusters with new ligand species, and by the availability of thin film ablation techniques in our research group, we have decided to investigate *mixed ligand* sandwich species. As shown in the following, mixed ligand complexes containing benzene, C_{60}, or coronene are produced conveniently from a pulsed nozzle cluster source using the thin film-plus-metal ablation method. We then investigate the photodissociation of these complexes to explore relative metal–ligand bond energies. Competitive ligand binding is a well established method with which to order binding energies. Metal ligand bond energies are not available for any of these new complexes, and this information bears critically on the future prospects for the isolation of such species in macroscopic quantities. As described, trends in cluster growth and dissociation establish a hierarchy of binding energetics for these three ligands with iron.

2. Experimental

Mixed ligand complexes of iron with benzene, coronene, and C_{60} are produced in a laser vaporization cluster source with specially prepared samples, as described previously [37]. Coronene and/or C_{60} are applied as thin films via sublimation onto an iron rod using a small vacuum chamber dedicated for sample preparation. For benzene/C_{60} or benzene/coronene mixtures, the film is pure C_{60} or pure coronene, respectively, and benzene is seeded in the expansion gas near its room temperature vapor pressure. For C_{60}/coronene mixtures, both components are deposited in the same thin film. Films of coronene or C_{60} have essentially zero vapor pressure at room temperature and are stable in vacuum for long periods.

The film coated sample rod is transferred to a molecular beam machine and mounted in a laser vaporization cluster source. This source uses a modified Newport nozzle [39]. Vaporization is accomplished with the third harmonic of a Nd:YAG laser at 355 nm. The conditions are similar to those recently described for Ag_x–C_{60} complex formation where signals are sensitive to both film thickness and the vaporization laser power [37]. Under optimized conditions the vaporization laser desorbs the film and penetrates through to ablate the underlying metal, thus producing the film component(s) and metal in the gas phase, which recombine in the growth channel of the source. The expanding gas mixture passes through a skimmer and cations are extracted from the molecular beam into the mass spectrometer with pulsed acceleration voltages. The beam apparatus for these experiments was described previously [10–12].

Cluster ions are mass selected with a specially designed reflectron time-of-flight mass spectrometer for photodissociation studies [10–12]. A pulsed deflection plate located at the end of the first flight tube transmits only the ions of interest, which are then excited with a pulsed Nd:YAG laser (532 or 355 nm) in the turning region of the reflectron field. The time of flight through the second arm of the reflectron determines the masses of photofragments.

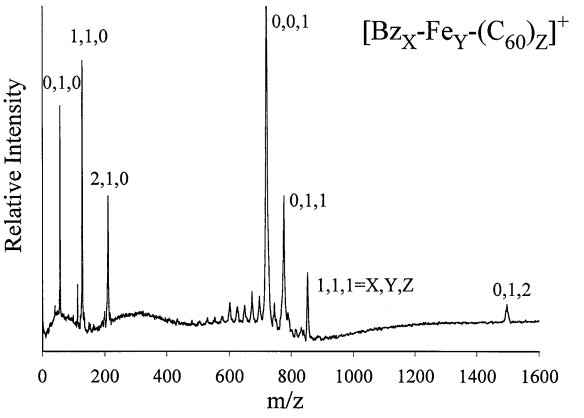

Fig. 1. The mass distribution of cations produced for the mixture of benzene and C_{60} with iron. An iron rod coated with a film of C_{60} is ablated in an expansion of helium seeded with benzene to produce this spectrum.

3. Results and discussion

Figs. 1–3 show the mass distributions produced for iron with the ligands benzene, coronene, and C_{60} taken in pairs. These spectra are produced by sampling the cations that grow in the source out of the molecular beam into the mass spectrometer without any postsource ionization. The source conditions (channel diameter and length) are adjusted to minimize the formation of pure iron clusters and to

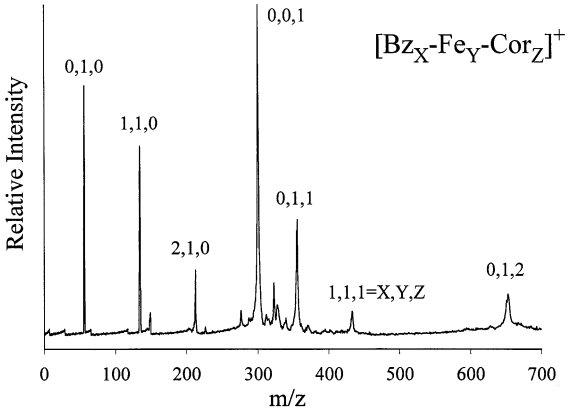

Fig. 2. The mass distribution of cations for the mixture of benzene and coronene with iron. An iron rod coated with a film of coronene is ablated in an expansion of helium seeded with benzene to produce this spectrum.

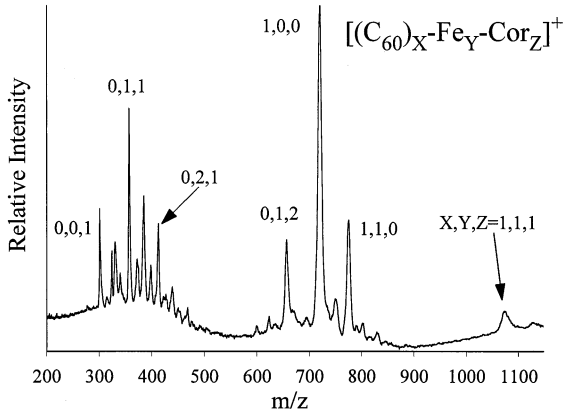

Fig. 3. The mass distribution of cations produced for the mixture of coronene and C_{60} with iron. Coronene and C_{60} are deposited in a mixed thin film on the surface of an iron rod and subjected to laser ablation to produce this spectrum.

promote the formation of metal complexes, as described previously [25,37]. The intensities therefore should represent the relative concentrations of the species grown, assuming no significant mass discrimination over this range. Mass discrimination is impossible to eliminate completely, and therefore we do not report quantitative intensities. An additional concern is that these spectra not be biased too much by the relative concentrations of the ligands present. Control of ligand concentration is extremely difficult when components are added from both gas phase sources and ablated films. Therefore, we make random variations in both components (via film concentration, ablation laser power, pulsed nozzle backing pressure, benzene reservoir temperature, etc.) until the mass spectra indicate that both ligand species are present in the complex ions observed. It is still impossible to make quantitative comparisons of relative complex concentrations because the amounts of ionized versus neutral ligands is unknown.

Figure 1 shows the mass distribution of iron complexes with benzene and C_{60}. Prominent cation masses include Fe^+, $[Fe–benzene]^+$, $[Fe–benzene_2]^+$, C_{60}^+, $[Fe–C_{60}]^+$, $[benzene–Fe–C_{60}]^+$, and $[Fe–(C_{60})_2]^+$. Unlabeled smaller masses here (and in Figs. 2 and 3) are due to oxide and/or alkali metal impurities as well as a small amount of ligand fragment ions. Benzene is not observed as an isolated

Table 1
Ionization energies and dissociation energies relevant for this study

Atom/molecule	IE (eV)	$D_0(Fe–ligand)^+$ (kcal/mol)
Fe	7.87	...
Benzene	9.24	48,[a] 49[b]
Coronene	7.29	>32[c]
C_{60}	7.58	...

[a] [17].
[b] [14].
[c] [24].

cation, but instead must be present as a neutral species in the plasma. Because it is added as a gas phase component, its concentration is probably greater than that of the ablated C_{60}. Presumably, if benzene becomes ionized it undergoes effective charge transfer with other plasma components because of its relatively high ionization energy (see Table 1). The significant intensity of benzene-containing mass peaks and that for C_{60} itself indicate that both ligands are present in reasonable concentrations. Significantly, there is very little evidence for fragmentation of the benzene and C_{60} ligand species. A small amount of fragmentation is evident below the C_{60}^+ mass, where the usual C_2 loss pattern is seen. However, all prominent masses correspond to whole units of these ligands either alone or added to the metal.

Significantly, there are no masses observed corresponding to benzene clusters, $(C_{60})_N$ clusters or benzene–C_{60} complexes without iron. Such nonmetal molecular complexes, in both charged and neutral forms, can be produced in our beam machine using a different nozzle configuration which makes a colder supersonic expansion. The present configuration (long gas channel/large diameter bore) makes essentially no weakly bound ion–molecule clusters. It also makes essentially no pure iron clusters without ligands, presumably due to the lower average density of metal. These conditions were discussed previously in our work on iron–coronene clusters [25]. The absence of molecular clusters under these conditions provides strong evidence that the benzene–Fe–benzene, C_{60}–Fe–C_{60}, and benzene–Fe–C_{60} masses observed represent *sandwich* structures. The masses detected could

also be consistent with Fe–benzene–benzene, Fe–C_{60}–C_{60}, Fe–benzene–C_{60}, or Fe–C_{60}–benzene structures. However, these latter species would have ligand–ligand bonding through weaker electrostatic interactions. If these kinds of structures are formed we would also expect to see some corresponding weakly bound species without iron, but we do not [40].

The peak intensities observed here are affected by the rate of binding iron to each respective ligand and the intrinsic stability of the Fe–benzene and Fe–C_{60} complexes. We would like to determine the relative thermochemistry. However, many variables affect the kinetics, and it is impossible to control these variables or separate their influences. Benzene and C_{60} have different collision cross sections and ionization energies, and therefore the collision rates and ionized fractions of these species in the plasma may be very different. Finally, the metal complex cations can grow from metal ions reacting with neutral ligands or from neutral metal reacting with charged ligands. Neutral reactions are generally slower than ion reactions, but complexes could also grow as neutrals and then be ionized in the plasma. The cation peak intensities are therefore not very useful in the determination of stabilities for these various sandwich complexes. However, these mass spectra do demonstrate that mixed ligand sandwiches form about as easily as homoligand sandwiches.

Figure 2 shows the same kind of mass distribution for the cation clusters which form from iron with benzene and coronene. Prominent masses in this spectrum are Fe^+, $[Fe–benzene]^+$, $[Fe–benzene_2]^+$, $coronene^+$, $[Fe–coronene]^+$, $[benzene–Fe–coronene]^+$, and $[Fe–coronene_2]^+$. Again, there is little evidence for ligand fragmentation. There are diligand and mixed ligand complexes with iron, but no molecular complexes without iron, as described for Fig. 1. We therefore conclude again that these diligand and mixed ligand iron complexes represent sandwich structures. The $[Fe–coronene_2]^+$ sandwich complex was investigated in our previous study of iron-coronene clusters [25]. It was found as the most abundant ion produced by the cluster source and it was the only fragment ion from larger Fe–$(coronene)_{N>2}$ cluster ions, and was thus concluded to have enhanced stability relative to other complexes.

The final combination of ligands is shown in Fig. 3 where the cation complexes produced from the coronene/C_{60} mixture is shown. In this case, since both species are produced by film ablation, it is likely that their concentrations are comparable. Prominent masses are observed for $coronene^+$, $[Fe–coronene]^+$, $[Fe–coronene_2]^+$, C_{60}^+, $[Fe–C_{60}]^+$, and $[C_{60}–Fe–coronene]^+$. Although this mass spectrum does not show it, no measurable intensity is detected in this particular experiment for $[Fe–(C_{60})_2]^+$. However, in experiments when the relative C_{60} concentration is greater, this mass is detected. As before, there is very little ligand fragmentation. The group of extra peaks near 300–400 amu represent alkali adducts to the coronene ligand and/or complex masses. As before, there are essentially no molecular complexes without iron (except for a very small amount of coronene dimer at 600 u), and we conclude again that these diligand and mixed ligand complexes are sandwiches. A small amount of Fe_2–coronene is indicated just above mass 400. This fascinating complex and Fe_3–coronene were investigated in our previous work [25] and both were concluded to represent structures with separated iron atoms binding on the coronene surface.

While the concentrations of both Fe–coronene and Fe–C_{60} ions are substantial, it is interesting to compare the intensities of these complexes to those of the isolated ligands. The C_{60} peak is perhaps a factor of 3 greater in intensity than that of Fe–C_{60}, whereas the Fe–coronene peak is about a factor of 2 greater in intensity than that of the coronene cation. If the cation ligand peaks represent the relative concentrations available for binding, then this comparison suggests that coronene binds to iron more effectively on average than C_{60} does.

In all three systems, then, mixed ligand sandwich complexes form readily with ion abundances comparable to the homoligand sandwich complexes. The qualitative sandwich structures for these mixed systems are appealing, as shown in Fig. 4. These species are not close-shelled like ferrocene or dibenzene chromium, but if the metal–ligand bonding in Fe^+–benzene can be considered representative (49 kcal/

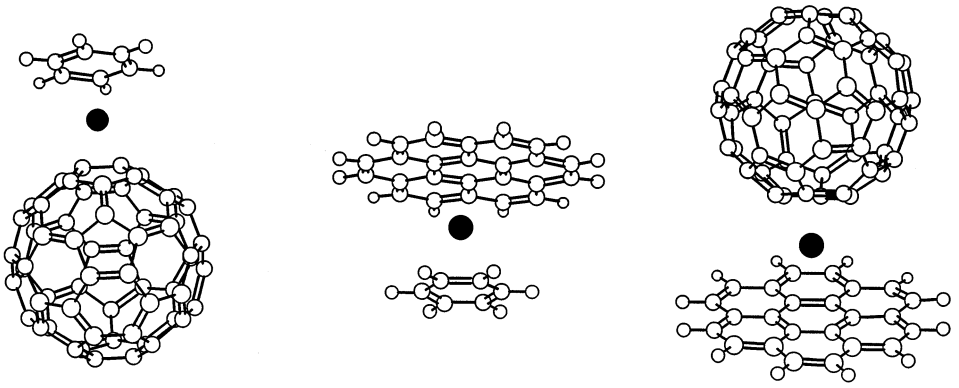

Fig. 4. The structures of mixed sandwich complexes suggested by the cation complex masses observed.

mol), the bond energies in these species may be substantial.

To investigate the relative strength of metal–ligand binding, we use photodissociation experiments on these mixed ligand complexes. If photodissociation occurs along the lowest energetic pathway, i.e. by internal conversion to the ground electronic state rather than out of an excited electronic state, then the weakest bond in the system should break first. The intramolecular bonds in these ligands are expected to be stronger than the metal–ligand bonds. In principle then, it should be possible to determine the primary dissociation channels in these mixed ligand complexes to identify the weaker of the two metal–ligand bonds. In other words, the ligand eliminated first represents the one with the weaker bond. Thus, even though we study the mixed ligand complexes, it is the stabilities of the final monoligand complexes which determine the outcome of the photodissociation. To ensure that photodissociation occurs in the ground state rather than in a specific excited state, we investigate photodissociation at more than one wavelength. This general procedure is essentially the "kinetic method" developed and applied to many ion–molecule complexes by Cooks and co-workers [41].

Fig. 5 shows the photodissociation mass spectra of the [benzene–Fe–C_{60}]$^+$ complexes at 355 and 532 nm. In this and other photodissociation spectra, the data are accumulated with a computer difference method. The mass spectrum measured with the fragmentation laser "off" is subtracted from that with the dissociation laser "on." The resulting spectrum shows the parent ion mass peak as a negative-going (depletion) peak, while the fragment ions produced are shown as positive peaks. As indicated, the photofragments detected are the same at both wavelengths. There is a small amount of [Fe–benzene]$^+$, but the most intense fragment is C_{60}^+. These fragmentation spectra are accumulated at relatively high laser power in order to see any signal at all. We therefore conclude that the dissociation process is multiphoton in nature. However, the data shown are studied as a function of laser power and the ratio of the two fragments

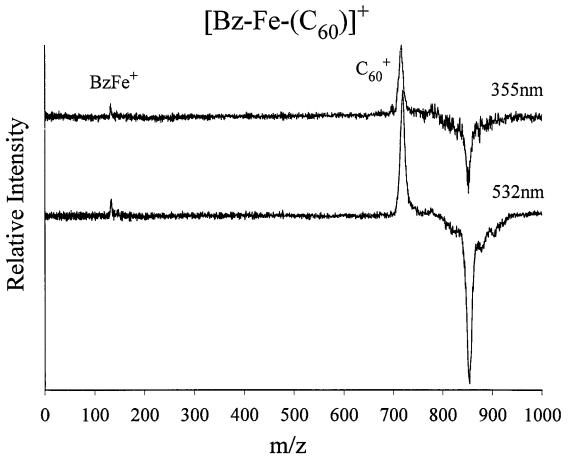

Fig. 5. The photodissociation mass spectrum of [benzene–Fe–C_{60}]$^+$ at 355 and 532 nm.

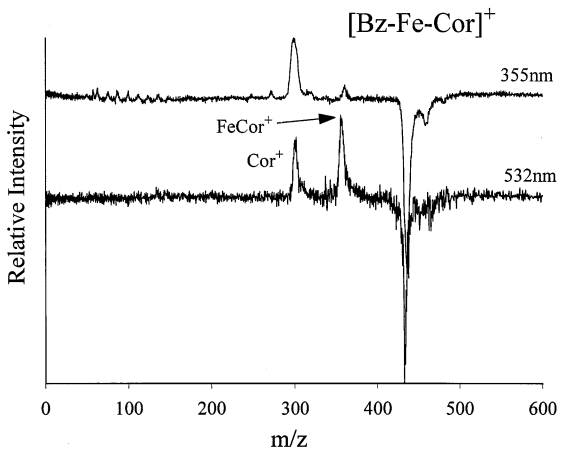

Fig. 6. The photodissociation mass spectrum of [benzene–Fe–coronene]$^+$ at 355 and 532 nm.

observed does not change with power. Additionally, no other fragments are observed at different powers. These same conditions are used to obtain the photodissociation spectra of [benzene–Fe–coronene]$^+$ and [C_{60}–Fe–coronene]$^+$, which are shown in Figs. 6 and 7.

Several observations are immediately evident from these photodissociation mass spectra for the mixed complex ions. First of all, there is no evidence of ligand fragmentation in any system. All fragmentation processes can be classified as simple ligand elimination. This is consistent with our earlier assumption

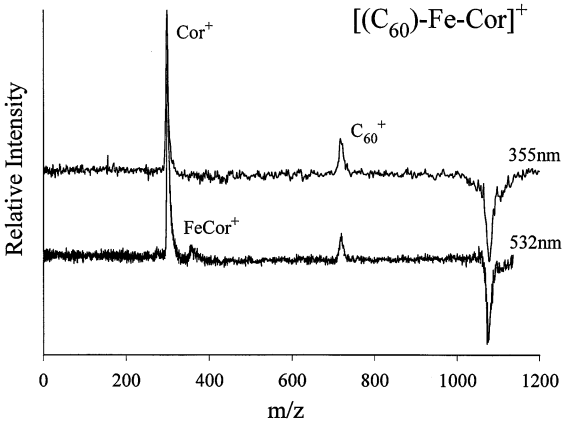

Fig. 7. The photodissociation mass spectrum of [C_{60}–Fe–coronene]$^+$ at 355 and 532 nm.

that metal–ligand bonds would be weaker than intraligand bonding. It also indicates that simple metal–ligand bonding occurs in these systems rather than metal insertion chemistry, and that our structural view of these complexes as mixed ligand sandwiches is correct. There are no fragmentation channels producing ligand–ligand fragment ions with loss of metal, again consistent with the picture of sandwich structures. All three mixed complexes are resistant to photofragmentation and require multiphoton laser conditions to accomplish dissociation on the time scale of our time-of-flight instrument (2–3 μs). This was also seen for several of the previously studied sandwich complexes with two of the same ligands. In particular, [Fe–coronene$_2$]$^+$ was especially difficult to fragment [25]. As noted before, this behavior is quite different from that of pure iron cluster cations, which fragment readily with one-photon at visible laser wavelengths [25]. These observations are consistent with relatively strong bonding for these complexes. Additionally, the inefficiency of the fragmentation argues strongly against excited state photochemistry. If dissociation takes place in an excited state pumped directly by the laser, the bond-breaking should be prompt and the process should be relatively efficient, as is observed for pure iron clusters. Increasing the laser intensity should produce a linear increase in signal. Inefficient dissociation, with a nonlinear power dependence as observed here, implies that internal conversion to the ground electronic state takes place and that additional energy from multiphoton absorption is required to make the rate of fragmentation fast enough to measure.

To examine these fragmentation processes in more detail, it is necessary to carefully consider the ionization energies (IEs) of the ligands and how these affect the dissociation processes (see Table 1). This is demonstrated more clearly by the consideration of monoligand complexes. For example, [Fe–coronene]$^+$ has been observed to photodissociate to neutral iron atoms and charged coronene [25]. Dissociation to produce ionized iron and neutral coronene is not observed because the ionization energy of coronene is much lower than that of iron. Likewise, dissociation of [Fe–C_{60}]$^+$ also produces neutral iron

and charged C_{60} for the same reason. On the other hand, dissociation of $[Fe–benzene]^+$ produces charged iron and neutral benzene because the IE of iron is lower than that of benzene. This general behavior, where the lower IE species carries the charge, is expected for the dissociation of ionized complexes except in special cases where photoinduced charge transfer may be observed [10,11]. Ionization energies also determine the charge distribution within complexes. For example, in $[Fe–benzene]^+$, the charge is expected to reside primarily on the iron atom. In $[Fe–C_{60}]^+$ and $[Fe–coronene]^+$, it should reside mostly on the ligand, but there will be more delocalization because the IEs are closer.

With these concepts in mind, the decomposition of these mixed complexes can be considered. The fragmentation of $[benzene–Fe–C_{60}]^+$, which produces only C_{60}^+ and $[Fe–benzene]^+$ as charged fragments, can be explained by consideration of the following channels:

$$[benzene–Fe–C_{60}]^+ \rightarrow Fe–benzene + C_{60}^+ \quad (1)$$

$$[benzene–Fe–C_{60}]^+ \rightarrow [Fe–benzene]^+ + C_{60} \quad (2)$$

$$[benzene–Fe–C_{60}]^+ \rightarrow benzene + [Fe–C_{60}]^+ \rightarrow Fe + C_{60}^+ \quad (3)$$

The branching into these particular charged and neutral fragments is expected because C_{60} [indicated as charged in reaction (1)] has a lower IE than either iron or benzene, while benzene [indicated as neutral in reaction (3)] has a higher IE than either iron or C_{60}. Reaction (1) is simple cleavage of the iron–C_{60} bond, producing C_{60}^+ directly. This reaction is expected if the iron–C_{60} bond is the weaker of the two metal–ligand interactions and if the IE of iron–benzene is greater than that of C_{60}. If the IE of Fe–benzene is about the same or lower than that of C_{60}, breakage of the iron–C_{60} bound would lead to reaction (2), which has the charged fragment $[Fe–benzene]^+$. If further fragmentation of Fe–benzene occurs in reaction (1), it would involve only neutral species and would be undetected. If further fragmentation of $[Fe–benzene]^+$ occurs in reaction (2), Fe^+ would result, but no Fe^+ is detected. Reaction (3) could also produce C_{60}^+ by a two step process involving breakage of the iron–benzene bond first followed by a second step which breaks the iron–C_{60} bond. This process would suggest an intermediate ion of $[Fe–C_{60}]^+$, which is also not detected. We therefore conclude that the primary dissociation process for $[benzene–Fe–C_{60}]^+$ is loss of C_{60} or C_{60}^+, as indicated in reactions (1) and (2). These combined channels explain both fragments observed and do not produce any ions that are not observed. Both channels correspond to elimination of C_{60} (neutral or charged), indicating that the iron–benzene bond is stronger than the iron–C_{60} bond in this cation complex.

Figure 6 shows the photodissociation of [benzene–Fe–coronene]$^+$ at 355 and 532 nm. In this case, the fragments observed have different intensities at the two wavelengths studied. Both spectra show the fragment ions $[Fe–coronene]^+$ and coronene, but the relative amount of $[Fe–coronene]^+$ is much less at 355 nm. There are two fragmentation channels to consider to interpret these spectra

$$[benzene–Fe–coronene]^+ \rightarrow benzene + [Fe–coronene]^+ \rightarrow coronene^+ + Fe \quad (4)$$

$$[benzene–Fe–coronene]^+ \rightarrow coronene^+ + Fe–benzene \quad (5)$$

Only these specific charged and neutral fragments are considered because of the IE trends. In reaction (4), benzene is ejected first and the coronene cation is formed by continued fragmentation of the intermediate $[Fe–coronene]^+$ ion. In reaction (5), the coronene ion is produced directly. Since we observe the $[Fe–coronene]^+$ ion expected as an intermediate in reaction (4), and since the ratio of this intermediate changes with the laser energy, a sequential fragmentation process is indicated. Thus, we can conclude that reaction (4) represents the primary dissociation of $[benzene–Fe–coronene]^+$ and that the metal benzene bond breaks first in this system. This suggests that the iron–coronene bond is stronger than the iron–benzene bond in this cation complex.

Figure 7 shows the photodissociation spectrum of

$[C_{60}–Fe–coronene]^+$. The spectrum is again the same at both 355 and 532 nm. The fragment ions observed are $coronene^+$, C_{60}^+ and a small amount of $[Fe–coronene]^+$. The expected fragmentation pathways are

$$[C_{60}–Fe–coronene]^+ \rightarrow C_{60} + [Fe–coronene]^+ \rightarrow coronene^+ + Fe \quad (6)$$

$$[C_{60}–Fe–coronene]^+ \rightarrow C_{60}^+ + Fe–coronene \quad (7)$$

$$[C_{60}–Fe–coronene]^+ \rightarrow coronene^+ + Fe–C_{60} \quad (8)$$

$$[C_{60}–Fe–coronene]^+ \rightarrow coronene + [Fe–C_{60}]^+ \rightarrow C_{60}^+ + Fe \quad (9)$$

In this system, more reactions are considered because the ionization energetics are less certain. Thus, reactions (6)–(9) are the same except for the charge branching. Since iron has a higher IE than C_{60} but coronene has a lower IE than C_{60}, it is likely that C_{60} and Fe–coronene have IEs close in energy. Reaction (9) is not likely because coronene has a lower IE than either C_{60} or iron. As indicated, the coronene cation, which is observed as the largest fragment ion, can occur from direct or sequential fragmentation processes in reactions (6) or (9), respectively. However, these two production schemes lead to very different conclusion about the relative metal–ligand bonding. The C_{60}^+ fragment can only occur from reaction (7) or (unlikely) reaction (9). Reaction (6) produces $[Fe–coronene]^+$ as an intermediate, and this is also detected. To explain both the C_{60}^+ and $[Fe–coronene]^+$ fragments, therefore, we conclude that a combination of reactions (6) and (7) are likely going on in parallel for this system. This suggests that the IEs for C_{60} and [Fe–coronene] are indeed close in energy. Thus, the iron–C_{60} bond breaks and the stronger Fe–coronene bond is retained. This same result would have been predicted from the bond energy trends already obtained from the analysis of Figs. 5 and 6.

The three combined photodissociation processes indicate the following trend in ligand bond energies to iron in these cation complexes: coronene > benzene > C_{60}. There is one caveat to this conclusion, however. The charge distributions in the mixed ligand complexes make it impossible to compare exactly the same bond breaking in each system. Thus, when $[benzene–Fe–coronene]^+$ dissociates as in Fig. 6, the wide IE difference between coronene, iron and benzene indicates that the charge is somewhat more localized on the coronene molecule, i.e. benzene–Fe–$coronene^+$. Then, when photoexcitation induces competitive bond breaking, we are comparing the more neutral iron–benzene interaction to the more charged iron–coronene interaction. This same issue of charge distribution is present in each of the three mixed ligand dissociation processes studied. However, it is not easy to predict how the metal–ligand bond energy is affected by these charge differences. In every case, the iron atom is more nearly neutral, while the charge is expected to be more localized on a low IE ligand (coronene or C_{60}). Both coronene and C_{60} have large π-bonding networks, and so the charge will be delocalized on these ligands. It may turn out, then, that the interactions studied here for cations are not very different from those in the corresponding neutral systems (which unfortunately cannot be studied). To further investigate this possibility, it would of course be interesting to measure specific metal–ligand bond energies by studying the individual single-ligand cation complexes. The difficulty in fragmenting these species with light indicates that a threshold photodissociation experiment does not hold much promise for these measurements. However, collisional dissociation thresholds for the individual single-ligand complexes would perhaps be useful in this regard. The Fe^+–benzene bond energy is 49 kcal/mol [14]. Our data here implies that the $[Fe–coronene]^+$ bond energy is greater than this value and that the $[Fe–C_{60}]^+$ bond energy is less than this value. Pozniak and Dunbar [24] have bracketed the bond energy of $[Fe–coronene]^+$ to be greater than 32 kcal/mol, which is consistent with our result.

The trend in iron–ligand bond energies suggested here is sensible, and can be understood by consideration of traditional transition metal complexes. By this reasoning, the $[Fe–benzene]^+$ complex has seven metal electrons and six π electrons from the single

benzene ligand, and is therefore electron deficient. The bonding is enhanced with the coronene ligand which has a more extensive π cloud to donate a more effective charge to the iron orbitals. Thus, coronene binds stronger than benzene to iron. In the case of C_{60}, the curved surface leads to poorer π bonding and there is effectively less charge donation to the metal, resulting in weaker bonding. More detailed ab initio calculations would of course be of interest to shed light on the nature of bonding in these systems.

4. Conclusions

The mixed ligand complexes [benzene–Fe–C_{60}]$^+$, [benzene–Fe–coronene]$^+$, and [C_{60}–Fe–coronene]$^+$ are produced by laser ablation of film coated iron samples in a pulsed nozzle source. Benzene is seeded in the expansion gas when required. These mixed ligand sandwich complexes are produced with comparable abundance to the corresponding homoligand sandwich complexes, which have been studied previously. Mass spectra show that the production of these complexes is clean with little evidence for reactive or plasma-induced fragmentation processes. The conditions of the experiment and the details of the mass spectra provide strong evidence that these are sandwich complexes. Similar film ablation techniques may be useful for the production of a variety of organometallic complexes with other ligands.

Mass-selected photodissociation experiments on these complexes show simple elimination of ligands, which suggests that there is straightforward metal–ligand bonding without metal insertion chemistry. Dissociation is relatively inefficient and requires high intensity laser excitation, consistent with unimolecular dissociation in the ground electronic state rather than excited state photochemistry. Under these conditions, dissociation should follow the lowest energy pathways, and more weakly bound ligands should be preferentially eliminated. Ligand elimination patterns suggest that the relative strengths of ligand binding to iron in these cation complexes are coronene $>$ benzene $>$ C_{60}. This pattern of bonding is consistent with expectations based on the relative densities of ligand π electrons which are available for donation to the iron orbitals. Future studies may use these bonding concepts to design novel sandwich complexes with enhanced stability.

Acknowledgements

We gratefully acknowledge support for this work from the National Science Foundation (grant no. CHE-9529043) and the Air Force Office of Scientific Research (grant nos. F49620-97-1-0042 and F49620-97-1-0386). We appreciate helpful discussions with Dr. Charles Kutal, Dr. Bruce King, and Dr. James Fye. We dedicate this paper to the memory of Ben Freiser who was a good friend and colleague. Much of our work in organometallic ion–molecule chemistry was inspired by his previous contributions in this area.

References

[1] R.S. Mulliken, W.B. Person, Molecular Complexes, Wiley-Interscience, New York, 1969.
[2] J.C. Ma, D.A. Dougherty, Chem. Rev. 97 (1997) 1303.
[3] D.A. Dougherty, Science 271 (1996) 163.
[4] J.W. Caldwell, P.A. Kollman, J. Am. Chem. Soc. 117 (1995) 4177.
[5] Gas Phase Inorganic Chemistry, D.H. Russell (Ed.), Plenum, New York, 1989.
[6] D.B. Jacobson, B.S. Freiser, J. Am. Chem. Soc. 106 (1984) 3900.
[7] D.B. Jacobson, B.S. Freiser, J. Am. Chem. Soc. 106 (1984) 4623.
[8] D. Rufus, A. Ranatunga, B.S. Freiser, Chem. Phys. Lett. 233 (1995) 319.
[9] S. Afzaal, B.S. Freiser, Chem. Phys. Lett. 218 (1994) 254.
[10] K.F. Willey, P.Y. Cheng, M.B. Bishop, M.A. Duncan, J. Am. Chem. Soc. 113 (1991) 4721.
[11] K.F. Willey, C.S. Yeh, D.L. Robbins, M.A. Duncan, J. Phys. Chem. 96 (1992) 9106.
[12] D.S. Cornett, M. Peschke, K. LaiHing, P.Y. Cheng, K.F. Willey, M.A. Duncan, Rev. Sci. Instrum. 63 (1992) 2177.
[13] Y.M. Chen, P.B. Armentrout, Chem. Phys. Lett. 210 (1993) 123.
[14] F. Meyer, F.A. Khan, P.B. Armentrout, J. Am. Chem. Soc. 117 (1995) 9740.
[15] M. Sodupe, C.W. Bauschlicher, J. Phys. Chem. 95 (1991) 8640.
[16] M. Sodupe, C.W. Bauschlicher, S.R. Langhoff, H. Partridge, J. Phys. Chem. 96 (1992) 2118.

[17] C.W. Bauschlicher, H. Partridge, S.R. Langhoff, J. Phys. Chem. 96 (1992) 3273.
[18] M. Sodupe, C.W. Bauschlicher, Chem. Phys. 185 (1994) 163.
[19] R.C. Dunbar, S.J. Klippenstein, J. Hrusak, D. Stöckigt, H. Schwartz, J. Am. Chem. Soc. 118 (1996) 5277.
[20] Y.P. Ho, Y.C. Yang, S.J. Klippenstein, R.C. Dunbar, J. Phys. Chem. 101 (1997) 3338.
[21] K. Hoshino, T. Kurikawa, H. Takeda, A. Nakajima, K. Kaya, J. Phys. Chem. 99 (1995) 3053.
[22] K. Judai, M. Hirano, H. Kawamata, S. Yabushita, A. Nakajima, K. Kaya, Chem. Phys. Lett. 270 (1997) 23.
[23] P. Weis, P.R. Kemper, M.T. Bowers, J. Phys. Chem. A 101 (1997) 8207.
[24] B.P. Pozniak, R.C. Dunbar, J. Am. Chem. Soc. 119 (1997) 10439.
[25] J.W. Buchanan, J.E. Reddic, G.A. Grieves, M.A. Duncan, J. Phys. Chem. 102 (1998) 6390.
[26] J.W. Buchanan, G.A. Grieves, N.D. Flynn, M.A. Duncan, Int. J. Mass Spectrom. Ion Process, in press.
[27] L.M. Roth, Y. Huang, J.T. Schwedler, C.J. Cassady, D. Ben-Amotz, B. Kahr, B.S. Freiser, J. Am. Chem. Soc. 113 (1991) 6298.
[28] Y. Huang, B.S. Freiser, J. Am. Chem. Soc. 113 (1991) 8186.
[29] Y. Huang, B.S. Freiser, J. Am. Chem. Soc. 113 (1991) 9418.
[30] Q. Jiao, Y. Huang, S.A. Lee, J.R. Gord, B.S. Freiser, J. Am. Chem. Soc. 114 (1992) 2726.
[31] Y. Basir, S.L. Anderson, Chem. Phys. Lett. 243 (1995) 45.
[32] M. Welling, R.I. Thompson, H. Walther, Chem. Phys. Lett. 253 (1996) 37.
[33] T.P. Martin, N. Malinowski, U. Zimmermann, U. Naher, H.J. Schaber, J. Chem. Phys. 99 (1993) 4210.
[34] U. Zimmermann, N. Malinowski, U. Naher, S. Frank, T.P. Martin, Phys. Rev. Lett. 72 (1994) 3542.
[35] F. Tast, N. Malinowski, S. Frank, M. Heinebrodt, I.M.L. Billas, T.P. Martin, Phys. Rev. Lett. 77 (1996) 3529.
[36] F. Tast, N. Malinowski, M. Heinebrodt, I.M.L. Billas, T.P. Martin, J. Chem. Phys. 106 (1997) 9372.
[37] J.E. Reddic, J.C. Robinson, M.A. Duncan, Chem. Phys. Lett. 279 (1997) 203.
[38] A. Nakajima, S. Nagao, H. Takeda, T. Kurikawa, K. Kaya, J. Chem. Phys. 107 (1997) 6491.
[39] L.R. Brock, J.S. Pilgrim, D.L. Robbins, M.A. Duncan, Rev. Sci. Instrum. 67 (1996) 2989.
[40] In strong contrast to the iron complexes discussed here and in our previous work, silver–coronene complexes only form when colder supersonic expansion conditions are employed [26]. Species such as $[Ag–coronene_N]^+$ fragment to produce $(coronene)_N^+$ ions, with the loss of silver. There is then evidence that some silver–coronene complexes have structures other than sandwiches.
[41] R.G. Cooks, J.S. Patrick, T. Kotiaho, S.A. McLuckey, Mass Spectrom. Rev. 13 (1994) 287.